Toxicon 267 (2025) 108590

Contents lists available at ScienceDirect

Toxicon

journal homepage: www.elsevier.com/locate/toxicon

Short communication

Myotoxin II, a snake venom Lys49 phospholipase A_2 homolog, induces activation of the ryanodine receptor in artificial bilayers

Peter Szentesi [a,b,1,*], Zsuzsanna É. Magyar [a,b,1], Julián Fernández [c], László Csernoch [a,b], Marco Ruiz-Campos [c], Bruno Lomonte [c], José María Gutiérrez [c], Alfredo Jesús Lopez-Dávila [d,**]

[a] Department of Physiology, Faculty of Medicine, University of Debrecen, Debrecen, Hungary
[b] HUNREN-UD Cell Physiology Research Group, Debrecen, Hungary
[c] Instituto Clodomiro Picado, Facultad de Microbiología, Universidad de Costa Rica, San José, 11501, Costa Rica
[d] Institute of Molecular and Cell Physiology, Hannover Medical School, Carl-Neuberg-Str. 1, 30625, Hannover, Germany

ARTICLE INFO

Handling editor: Ray Norton

Keywords:
Ryanodine receptor
Single-channel
Sarcoplasmic reticulum
Mt-II

ABSTRACT

Envenomation by viperid snakes causes acute muscle tissue injury (myonecrosis). An important group of myotoxic components comprises catalytically-inactive Lys49 phospholipase A_2 homologs, which disrupt the integrity of the plasma membrane of skeletal muscle fibers through a mechanism that does not involve phospholipid hydrolysis. However, it remains unknown whether other mechanisms are involved in the cytotoxic action of these myotoxins. In this work, isolated calcium release channels (ryanodine receptor, RyR1) incorporated into an artificial lipid bilayer were used to study the action of the Lys49 phospholipase A_2 homolog myotoxin II (Mt-II) from the venom of *Bothrops asper*. Mt-II induced a dose-dependent activation of the RyR1. The open probability of the channel increased with the dose of the toxin. The maximal conductance of the channel remained unchanged during the toxin treatment. Furthermore, the analysis of the open and closed states showed a slight toxin dependency of the latter. These findings suggest that, in addition to the calcium influx from the extracellular space through the disrupted plasma membrane, Ca^{2+} release from the internal stores may also occur. However, incubation of C2C12 myotubes in culture with the RyR1 antagonist dantrolene did not reduce the extent of cytotoxicity induced by Mt-II, suggesting that the RyR1-mediated increase in cytosolic Ca^{2+} does not contribute to the overall myotoxicity of this toxin.

Envenomation by viperid snakes is often associated with pronounced skeletal muscle necrosis, which may lead to permanent tissue damage and disability (Gutierrez et al., 2017). The pathogenesis of acute muscle damage is associated with the synergistic action of myotoxic catalytically-active phospholipases A_2 (PLA_2s) and catalytically-inactive PLA_2 homologs (Lomonte, 2023; Mora-Obando et al., 2014). The latter, which include isoforms in which the canonical catalytic residue Asp49 has been substituted by Lys, induce cytotoxicity by penetrating and disorganizing the structure of the membrane phospholipid bilayer in the absence of phospholipid hydrolysis (Lomonte, 2023). A Lys49 PLA_2 homolog from the venom of the Central American viperid snake *Bothrops asper*, known as myotoxin II (Mt-II), is a model to investigate the mechanism of action of this family of myotoxins (Lomonte and Gutierrez, 1989).

It has been postulated that the key event in the cytotoxic action of these toxins is the disruption of the integrity of the skeletal muscle plasma membrane, with the consequent influx of extracellular calcium, which causes multiple deleterious effects leading to necrosis (Gutierrez and Ownby, 2003; Lomonte, 2023). However, the observation that myotoxins are internalized (Massimino et al., 2018; Vargas-Valerio et al., 2021) raises the possibility that these toxins may also affect intracellular targets such as mitochondria and sarcoplasmic reticulum (Montecucco et al., 2008). In the case of neurotoxic PLA_2s, it has been shown that they are internalized in the nerve terminal, affecting intracellular structures as part of their mechanism of action (Sribar et al., 2014). Thus, it is relevant to study the action of myotoxins on the

* Corresponding author. Department of Physiology, Faculty of Medicine, University of Debrecen, Debrecen, Hungary.
** Corresponding author. Institute of Molecular and Cell Physiology, Hannover Medical School, Hannover, Germany.
E-mail addresses: szentesi.peter@med.unideb.hu (P. Szentesi), lopezdavilacr@yahoo.es (A.J. Lopez-Dávila).
[1] Contributed equally to this work.

https://doi.org/10.1016/j.toxicon.2025.108590
Received 2 June 2025; Received in revised form 17 September 2025; Accepted 18 September 2025
Available online 20 September 2025

sarcoplasmic reticulum (SR) owing to the role of this organelle in intracellular calcium homeostasis. In this communication, we describe the action of *B. asper* Mt-II on the ryanodine receptor (RyR1), the calcium release channel of SR in skeletal muscle, incorporated into artificial bilayers.

The animal experiments followed the guidelines of the European Community (210/63/EU). The experimental protocol was approved by the Institutional Animal Care Committee of the University of Debrecen (3–1/2019/DEMAB).

1. Materials

Phospholipids were obtained from Avanti Polar Lipids, Inc. (Alabaster, AL). If not specified, all other chemicals were purchased from Sigma-Aldrich (St. Louis, MO).

2. Myotoxin II purification

A lyophilized pool of venoms from *Bothrops asper* adult specimens kept at Instituto Clodomiro Picado was used to isolate Mt-II (Uniprot P24605). Venom was dissolved in 0.1 M Tris, 0.1 M KCl (pH 7.0), subjected to cation-exchange chromatography on CM-Sephadex C25 (20 × 2 cm column equilibrated in the same buffer) and monitored at 280 nm (Lomonte and Gutierrez, 1989). A flow rate of 0.4 mL/min was used. After elution of unbound proteins, a linear gradient towards 0.1 M Tris, 0.75 M KCl (pH 7.0) was applied. The last eluting peak was collected, dialyzed, lyophilized, and stored at −20 °C. The deconvoluted monoisotopic intact mass of the protein was determined to confirm the identity of the protein, by direct infusion to a Q-Exactive Plus (Thermo) mass spectrometer. The effect of Mt-II on RyR1 electric currents was characterized by applying Mt-II concentrations of 50, 100 and 150 μg/mL. These concentrations correspond to 3.6, 7.3 and 10.9 μM, respectively. The cytotoxic effect of Mt-II on C2C12 myotubes was characterized by applying 200 μg/mL Mt-II, corresponding to 14.5 μM. The monomeric molecular weight of Mt-II has been determined to be 13750 Da (Lomonte and Fernandez, 2022).

3. Ryanodine receptor purification

Skeletal muscle tissue (25 g) was collected from wild-type, mixed-gender BL6 mice (2–5 months old, weighing 20–30 g). Mice were euthanized by CO_2 anaesthesia, followed by cervical dislocation. The muscle tissue was then dissected using scissors and forceps. All steps of the purification protocol were performed on ice or at 4 °C in the presence of protease inhibitors (pefabloc SC, aprotinin, leupeptin, benzamidine, pepstatin A, and calpain inhibitor) to prevent protein degradation. The muscle samples, pooled from 10 mice, were homogenized in a buffer containing 100 mM NaCl, 20 mM EGTA, and 20 mM Na-HEPES (pH 7.5). Cellular debris was removed by centrifugation at 3500×*g* for 35 min. SR microsomes were isolated by differential centrifugation as follows. Initially, crude microsomes were collected from the supernatant by centrifugation at 40,000×*g* for 30 min using a Ti45 rotor. To eliminate actomyosin contamination, the pellet was resuspended in a buffer containing 600 mM KCl, 10 mM K-PIPES, 250 mM sucrose, 1 mM EGTA, and 0.9 mM $CaCl_2$ (pH 7.0) and incubated for 1 h. The microsomes were then collected by centrifugation at 109,000×*g* for 30 min. The resulting pellet was resuspended in 300 mM sucrose and 10 mM K-PIPES (pH 7.0), snap-frozen in liquid nitrogen, and stored at −70 °C until the solubilization step.

The microsomes were allowed to thaw on ice and subsequently solubilized in a buffer containing 1 % CHAPS, 1 M NaCl, 100 μM EGTA, 150 μM $CaCl_2$, 5 mM AMP, 0.45 % phosphatidylcholine, and 20 mM Na-PIPES (pH 7.2) for 2 h. The solubilized samples were then loaded onto a 10–28 % linear sucrose gradient and subjected to ultracentrifugation overnight at 90,000×*g* in an SW27 rotor. RyR1-containing fractions of the gradient were snap-frozen in liquid nitrogen and stored at −70 °C in small aliquots.

SDS-PAGE was used to verify the purified samples. 30 μl of each fraction (~400 μl) of the sucrose gradient was loaded into each 10 % linear gel well. Following electrophoresis, proteins were stained with Coomassie Brilliant Blue. Images were converted to black and white and were not further processed.

4. RyR1 reconstitution and single-channel current recording

Voltage-clamp measurements were performed on purified, single RyR1 channels incorporated into artificial planar lipid bilayers, as previously described (Lai et al., 1988). Bilayers were formed across an aperture with a diameter of 200 μm drilled in the wall of a Delrin cap (Warner Instruments, Hamden, CT), which separated two chambers. The chambers were filled with a recording solution containing: 250 mM KCl, 50 μM $CaCl_2$, 10 mM HEPES (pH 7.2). A small amount of purified RyR1 was added to the chamber, which was defined as the cis (cytoplasmic) side. The other chamber was considered the trans (luminal) side. Transmembrane voltages were referenced to ground (trans-to-cis), allowing ionic currents of physiological direction through open RyR1 channels. The free [Ca^{2+}] of the recording medium was adjusted using an EGTA stock solution.

The lipid mixture contained phosphatidylethanolamine (PE), phosphatidylserine (PS), and phosphatidylcholine (PC) (Avanti Polar Lipids, Alabaster, AL) in a ratio of 5:4:1. It was dissolved in *n*-decane at a final concentration of 20 mg/mL.

The currents through the RyR1 were recorded in voltage-clamp mode using an AxoPatch 200 amplifier and pCLAMP 6.03 (Axon Instruments, Sunnyvale, CA) software. The holding potential was −60 mV. To examine the voltage dependence of channel activation, the measurement was repeated in some cases at +60 mV. The currents were filtered at 1 kHz through an eight-pole low-pass Bessel filter and digitized at 3 kHz. The toxin was added to the cis chamber in increasing concentration.

5. Predicting the binding of Mt-II to RyR1

The possible binding of Mt-II to RyR1 was analyzed with the AlphaFold3 model (Abramson et al., 2024). AlphaFold Server is a web service (https://alphafoldserver.com) that can generate highly accurate biomolecular structure predictions containing proteins, ligands and ions. The interface predicted template modelling (ipTM) score was used to rank the binding of the two proteins. ipTM is derived from the template modelling score, which measures the accuracy of the entire structure (higher values predict better binding).

6. C2C12 cell culture and differentiation

C2C12 myoblasts (ATCC CRL-1772) were cultured utilizing high glucose Dulbecco's Modified Eagle Medium (DMEM) supplemented with 10 % Fetal Bovine Serum (FBS), sodium pyruvate (1 mM), L-glutamine (2 mM), penicillin (100 U/mL), streptomycin (100 μg/mL), and amphotericin B (0.25 μg/mL) (Thermo Fisher Scientific, Waltham, MA, USA). Confluent myoblast cultures were obtained and then differentiated to myotubes by employing a low-serum differentiation medium (high glucose DMEM, 1 % FBS, sodium pyruvate (1 mM), L-glutamine (2 mM), penicillin (100 U/mL), streptomycin (100 μg/mL), and amphotericin B (0.25 μg/mL) for 7 days. Cultures were maintained in an incubator at 37 °C and 5 % CO_2. Successful differentiation was determined by microscopic observation, i.e., the presence of multinucleated elongated myotubes.

7. Effect of dantrolene on the cytotoxic activity of myotoxin II on myotubes

In order to assess the role of the activation of RyR1 on the cytotoxic

activity of Mt-II on myotubes, approximately 1×10^4 myoblasts were seeded per well in a 96-well plate with 150 µL of culture medium and differentiated into myotubes as described above. To assess the inhibition of cytotoxicity by dantrolene, an inhibitor of RyR1, myotubes were incubated with either dantrolene (70 µM), dissolved in medium, or with medium alone. Incubation was carried out at 37 °C for 30 min. Then, Mt-II was added to myotube cultures (30 µg toxin per well) and incubated at 37 °C for 3 h. Cytotoxicity was assessed as previously described (Lomonte et al., 1999) by the quantification of lactic dehydrogenase (LDH) activity in the medium using a commercial kit (Cromatest, Wiener Lab, Rosario, Argentina). Each treatment was tested using triplicates, and each assay included a medium control (0 % cytotoxicity) and 100 % cytotoxicity control (0.1 % Triton X-100).

8. Statistics

Open probabilities (P_o) were determined using the pClamp software suite (Molecular Devices, Sunnyvale, CA). Results were expressed as mean ± standard error (SE). Relative P_o values were calculated by normalizing each data point to its corresponding control. All-point histograms were generated from 60-s-long recordings taken from representative datasets at the specified toxin concentration. This histogram represents the distribution of current amplitudes within the given current record, irrespective of the open/close state of the channel. These histograms were fitted with single exponentials, the averaged open and closed time constants (τ_o and τ_c) are given in the table of Fig. 1.

The effect of the toxin action on the open probability was analyzed with Hill's equation:

$$P_o = 1 + A\frac{X^n}{X^n + {K_d}^n} \qquad \text{Equation 1}$$

where X is the toxin concentration, K_d is the half-effective concentration of the toxin, and n is the Hill coefficient. The latter is a parameter that describes the degree of cooperativity in ligand binding to a protein, particularly in a multi-subunit protein like RyR1 (Meissner et al., 1997). Statistical analyses were performed using Prism software (GraphPad Software, San Diego, CA, USA). For comparisons between two groups, a two-tailed unpaired Student's t-test was used. For comparisons involving more than two groups, one-way analysis of variance (ANOVA) followed by Bonferroni's post hoc test was employed. A p-value of less than 0.05 was considered statistically significant. The number of observations in every condition is specified in the figure legends.

The effect of Mt-II on channel gating was studied using solubilized RyR1 from wild-type mice incorporated into an artificial planar lipid bilayer (Fig. 1A). Under control conditions, the RyR1 channel exhibits two states (open and closed). Increasing the toxin concentration further led to a gradual increase in the proportion of time the channel remained in the open state (Fig. 1B, C, 1D). The all-point histograms, which represent the frequency of events with a given amplitude, clearly demonstrate an increase in the number of open states as toxin concentration increases. The top peak in the histograms corresponds to the closed state (c), while the bottom peak represents the open state (o). Additionally, the amplitude of the open states gradually increased with higher toxin concentrations. This was confirmed by calculating the normalized open probability for each current trace. The single-channel open probability refers to the likelihood that a RyR1 is in the open state at any given time. The P_o increased with the toxin concentration from the control 0.08 (Fig. 1A) to 0.28 (150 µg/mL Mt-II, Fig. 1D). To compare the open probabilities from different measurements, the P_o in the control condition was considered 100 %, and the P_o calculated in the presence of different concentrations of the Mt-II was normalized to this. As shown in Fig. 1E, the average P_o increased with Mt-II concentration. The relationship between Mt-II concentration and P_o was fitted to Hill's equation (Equation (1)), yielding a half-maximal effective concentration (EC_{50}) of 74.5 µg/mL and a Hill coefficient of 4. This Hill coefficient suggests cooperative binding to RyR1. Finally, we analyzed the all-point histograms by fitting single exponential functions to calculate the closed and open times. The open and closed times describe the duration for which the channel remains in these respective states. The open probability is influenced by the channel's inherent properties and the

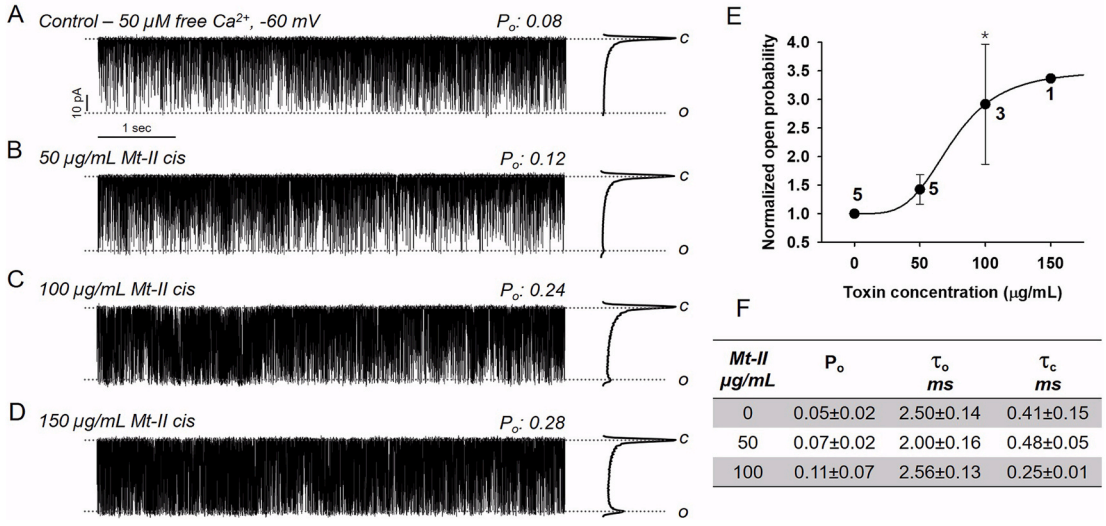

F

Mt-II µg/mL	P_o	τ_o ms	τ_c ms
0	0.05±0.02	2.50±0.14	0.41±0.15
50	0.07±0.02	2.00±0.16	0.48±0.05
100	0.11±0.07	2.56±0.13	0.25±0.01

Fig. 1. Mt-II increases the open probability of the RyR1.
A-D. Current traces of a single RyR1 channel under control conditions and in the presence of various concentrations of Mt-II. The solubilized RyR1 from wild-type mice was incorporated into an artificial planar lipid bilayer, and single-channel currents were recorded under voltage clamp conditions with a holding potential of −60 mV. The charge carrier was 250 mM KCl, with a symmetrical free calcium concentration of 50 µM. Channel openings are represented by downward deflections in the current traces. The open (o) and closed (c) states of the channel are marked on the right side of each current trace, accompanied by the corresponding all-point histograms for each recording at the specified Mt-II concentration.
E. Normalized and averaged open probabilities (P_o) as a function of Mt-II concentration. The numbers in the graph indicate the number of RyR1 channels measured. The dashed line represents the best fit of Hill's equation (Equation (1)), with the following parameters: A = 2.51, n = 3.99, and K_d = 74.50 µg/mL Asterisk (*) denotes a significant difference from control (0 µg/mL Mt-II; $p < 0.05$).
F. Table showing the averages of absolute open probability (P_o), open time (τ_o), and closed time (τ_c).

conditions it experiences, such as voltage and the presence of ligands. Open and closed times, on the other hand, reflect the kinetics of channel transitions between open and closed states. Thus, the increase found in P_o can be associated with either longer open times or shorter closed times. In our case the closed time decreased (Fig. 1F).

The voltage dependence of toxin action was tested with 50 μg/mL Mt-II. The open probabilities of RyR1 measured at −60 mV and +60 mV were compared. From four independent measurements, the average P_o normalized to the control open probability was 1.16 ± 0.12 and 1.00 ± 0.17 ($p > 0.9$) at −60 mV and +60 mV, respectively. Both values were not significantly different from the theoretical 1 ($p > 0.9$). The conductance of the channel was determined from current measurements at −60 mV and +60 mV, both in the absence and presence of 50 μg/mL Mt-II. Supplementary Fig. S1 displays the averaged currents along with the fitted linear functions. The average conductance under control conditions was 778.8 ± 9.2 pS, which was not significantly different ($p > 0.85$, $n = 4$) from the conductance measured in the presence of the toxin (775.3 ± 7.4 pS). The fitted lines passed close to the origin, indicating no voltage offset and confirming the accuracy of the conductance estimation, even when based on only two data points. As the ionic composition of the solution was symmetrical, no rectification or directionally biased conductance was expected. The slope of the I–V curve (I/U) corresponds to the conductance in pS, and the values obtained from the linear fits matched the averaged conductance values.

To assess whether the activation of RyR1 by Mt-II contributes to its cytotoxic activity on C2C12 myotubes, cells were incubated with dantrolene, an inhibitor of RyR1, before the addition of Mt-II to the cells. No decrease in cytotoxicity was observed when cells were pre-treated with dantrolene before Mt-II exposure, as compared to the control of Mt-II alone. Dantrolene alone induced a low extent of cytotoxicity, but it was significantly lower than in samples corresponding to myotubes incubated with Mt-II, either with or without pre-treatment with dantrolene (Fig. 2).

Our observations demonstrate that Mt-II induces a dose-dependent activation of the RyR1 in an artificial planar bilayer system. This finding suggests that once the toxin reaches the sarcoplasmic reticulum in skeletal muscle fibers, either by endocytosis or following the disruption of the plasma membrane, it may interact with and activate the RyR1, further contributing to the increased elevation of the cytosolic calcium concentration. Whether this effect plays a significant role in the overall cytotoxic effect of Mt-II remains to be elucidated. However, our experiments with dantrolene suggest that the activation of RyR1 induced by Mt-II does not contribute to its overall cytotoxic activity on myotubes, at least at the concentrations used in this study. Our findings agree with those of Rodrigues-Simioni et al., working with bothropstoxin, a similar Lys49 PLA_2 homolog (Rodrigues-Simioni et al., 1995). They reported that, while the toxin opened the RyR1 channel, dantrolene did not inhibit its deleterious action on skeletal muscle.

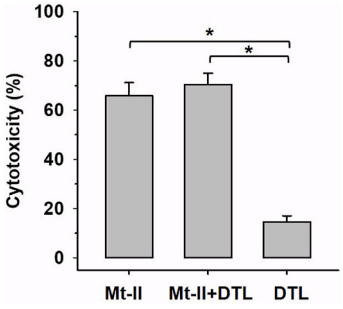

Fig. 2. Dantrolene does not reduce the cytotoxic activity of Mt-II in myotubes in culture.
C2C12 myotubes were incubated for 30 min at 37 °C with either dantrolene (DTL), dissolved in medium, or with medium alone. Then, Mt-II (30 μg/well) was added to the culture wells and cytotoxicity assessed by quantification of LDH release (see text for details). Cytotoxicity was expressed as a percentage, considering 100 % the LDH activity of samples incubated with 0.1 % Triton X-100. Controls included cells incubated with medium alone (corresponding to 0 % cytotoxicity) or with dantrolene alone. Bars represent the average ± SE of three replicates. *$p < 0.001$ when compared to the groups in which myotubes were incubated with Mt-II with or without inhibitors.

It is likely that, when the disruption of the plasma membrane by Mt-II is large enough, the prominent influx of calcium from the extracellular fluid overshadows the cytosolic increase of calcium mediated by the activation of the RyR1 channel. However, the possibility exists that in muscle cells in which the action of Mt-II on the plasma membrane is less pronounced, the opening of the RyR1 may have a higher contribution to cellular damage, thus expanding the action of the toxin.

One can expect a detrimental effect of Mt-II also on the artificial lipids used in our experiments. The lipid mixture was chosen primarily for practical reasons: to ensure stable incorporation and function of single RyR1 channels in an artificial bilayer system. While it includes lipids present in the SR (e.g., PS and PE), it is not intended to fully replicate the native SR or sarcolemmal membrane. Instead, it serves as a controlled model environment optimized for RyR1 reconstitution and functional analysis. The myotoxin did not affect the membrane containing the RyR1 in our experiments since a direct effect of Mt-II on the membrane used to place the RyR1 would induce spontaneous artefacts in the recordings. As demonstrated in Fig. 1, this was not the case. The absence of membrane alterations by the toxin is presumably attributable, at least in part, to the specific lipid composition of our bilayer. The skeletal sarcoplasmic reticulum has been found to be enriched in PC (~67 %) and PE (~16 %). In contrast, PS comprises approximately 11 % of the phospholipids. Furthermore, an asymmetrical distribution of phospholipids is observed between the inner and outer layers of the membrane, particularly in the cases of PE and PS (Bick et al., 1998). Conversely, the bilayer in our study comprised 50 % PE and 40 % PS (see above), in conjunction with symmetrically distributed phospholipids. This difference is likely to account for the lack of activity of the toxin on our lipid bilayer. Additionally, the unique ionic composition of the chamber surrounding the artificial planar bilayer may also influence the toxin's interaction with the lipid membrane. Therefore, our results do not constitute evidence that rules out an effect of Mt-II on the native sarcoplasmic reticulum membrane.

We analyzed the potential binding regions of Mt-II to RyR1. Initially, the full-length sequence of the human ryanodine receptor 1 (RyR1), consisting of 5038 amino acids (~565 kDa), was tested against Mt-II, a toxin composed of 122 amino acids (~14 kDa). This prediction attempt was unsuccessful, likely due to the large disparity in molecular weight and structural complexity between the two proteins. As a next step, we selected seven RyR1 domains previously identified as potential toxin-binding regions based on prior experimental data (Gaburjakova and Gaburjakova, 2023). These individual domains are comparable in size to Mt-II, and binding predictions with them were successful (Supplementary Table S1).

Among the tested regions, the handle domain and Chain A of RyR1 emerged as the most promising binding sites. The handle domain is located within the cytoplasmic region of RyR1 and plays a crucial role in channel gating and interdomain communication. It forms part of the large cytoplasmic assembly situated above the transmembrane pore-forming region and is involved in allosteric regulation, particularly in response to calcium and other modulators. Chain A represents one of the four identical subunits that comprise the RyR1 tetramer. Each subunit contains both N-terminal and C-terminal regions of the full protein. While Chain A itself does not have a unique functional role, it is essential for forming the complete channel pore. Both the handle domain and Chain A exhibit fourfold symmetry as part of the tetrameric structure (Yan et al., 2015). The Hill coefficient, derived from the open probability analysis, suggests cooperative binding of Mt-II to the tetrameric structure of RyR1. This is an aspect that should be the subject of further study. For the binding analysis, the human RyR1 sequence was employed, whereas the calcium release channel from the mouse was incorporated

into the lipid bilayer model. Despite the fact that mammalian RyR isoforms share approximately 88 % overall sequence identity (Tunwell et al., 1996), this level of conservation does not preclude species-specific differences in structural domains that may influence ligand interactions. Consequently, the results of the binding model may not fully recapitulate the behaviour observed in single-channel experiments and should be interpreted with caution. The human isoform of RyR1 used for the binding analysis is of particular interest from a translational perspective.

There is limited information on the interaction of venom toxins with RyR1. A peptide from a scorpion venom is a high-affinity activator of RyRs (Gurrola et al., 2010). In snake venoms, a glycosylated serine proteinase with thrombin-like activity from a viperid venom was shown to activate RyRs (Zeng et al., 2013). A cysteine-rich secretory protein (CRISP) from a cobra venom inhibits the binding of ryanodine to RyR1 and the calcium channel activity of RyR1 (Zhou et al., 2008). On the other hand, myotoxin *a*, a cationic peptide with myotoxic activity from rattlesnake venoms, induces calcium release from sarcoplasmic reticulum vesicles, but this action is not mediated by the RyR1 (Ohkura et al., 1995). Thus, a variety of animal venom components interact with RyRs in an example of functional convergent evolution. In the case of Mt-II, its mode of interaction with RyR1 deserves further studies.

Our results suggest that inhibiting RyR1 has little or no impact on reducing Mt-II toxicity in skeletal muscle. However, the activating effect of Mt-II on RyR1 could have practical applications beyond the study of snake venoms. These applications could include basic and translational research contexts. For instance, pathogenic variants of RyR1 can result in various muscle disorders. Some of these disorders are characterized by reduced Ca^{2+} release and force development during electrically evoked twitch stimulation (Liang et al., 2024). Furthermore, if Mt-II were to demonstrate an activating effect on the cardiac isoform of the receptor (RyR2), the scope of these applications would expand considerably. Some human RyR2 loss-of-function mutations are associated with a recently described cardiac arrhythmia disorder, termed RyR2 Ca^{2+}-release deficiency syndrome (CRDS). During *in vitro* characterization experiments, these mutated RyR2s exhibited reduced caffeine-induced Ca^{2+} release (Li et al., 2021). RyR1 and RyR2 are not only expressed in striated muscle but also in organs as diverse as the brain and pancreas, and targeting these and other ryanodine receptor isoforms has revealed a wide range of possibilities for treating human diseases (Marks, 2023).

In conclusion, *B. asper* Mt-II can induce activation of the RyR1 and might be a useful tool to study the physiology of the channel. However, our findings with myotubes in culture do not support a role of the opening of RyR1 on the cytotoxicity induced by this myotoxin. Therefore, the application of RyR1 blockers during Mt-II envenomation may not prevent its cytotoxic effect.

CRediT authorship contribution statement

Peter Szentesi: Writing – original draft, Visualization, Formal analysis, Data curation, Conceptualization. **Zsuzsanna É. Magyar:** Writing – original draft, Visualization, Investigation, Formal analysis, Data curation. **Julián Fernández:** Writing – review & editing, Validation, Resources, Methodology. **László Csernoch:** Writing – review & editing, Funding acquisition. **Marco Ruiz-Campos:** Writing – review & editing, Visualization, Investigation, Formal analysis. **Bruno Lomonte:** Writing – review & editing, Validation, Resources, Methodology. **José María Gutiérrez:** Writing – original draft, Validation. **Alfredo Jesús Lopez-Dávila:** Writing – review & editing, Validation, Supervision, Conceptualization.

Ethical statement

The animal experiments followed the guidelines of the European Community (210/63/EU). The experimental protocol was approved by the Institutional Animal Care Committee of the University of Debrecen (3–1/2019/DEMAB).

Declaration of competing interest

The authors declare the following financial interests/personal relationships which may be considered as potential competing interests:BL and JMG, given their role as members of the Editorial Board of Toxicon, had no involvement in the peer review of this article and had no access to information regarding its peer review. Full responsibility for the editorial process for this article was delegated to another journal editor. If there are other authors, they declare that they have no known competing financial interests or personal relationships that could have appeared to influence the work reported in this paper.

Acknowledgments

The research was financed by the project to L. Csernoch (no. K_137600), which has been implemented with the support provided by the Ministry of Innovation and Technology of Hungary from the National Research, Development and Innovation Fund, financed under the K_21 funding scheme. The support by Vicerrectoría de Investigación, Universidad de Costa Rica (741-B5-602) is also gratefully acknowledged. The last author is grateful to FX Kerschensteiner for long-standing support.

Appendix A. Supplementary data

Supplementary data to this article can be found online at https://doi.org/10.1016/j.toxicon.2025.108590.

Data availability

Data will be made available on request.

References

Abramson, J., Adler, J., Dunger, J., Evans, R., Green, T., Pritzel, A., Ronneberger, O., Willmore, L., Ballard, A.J., Bambrick, J., Bodenstein, S.W., Evans, D.A., Hung, C.C., O'Neill, M., Reiman, D., Tunyasuvunakool, K., Wu, Z., Zemgulyte, A., Arvaniti, E., Beattie, C., Bertolli, O., Bridgland, A., Cherepanov, A., Congreve, M., Cowen-Rivers, A.I., Cowie, A., Figurnov, M., Fuchs, F.B., Gladman, H., Jain, R., Khan, Y.A., Low, C.M.R., Perlin, K., Potapenko, A., Savy, P., Singh, S., Stecula, A., Thillaisundaram, A., Tong, C., Yakneen, S., Zhong, E.D., Zielinski, M., Zidek, A., Bapst, V., Kohli, P., Jaderberg, M., Hassabis, D., Jumper, J.M., 2024. Accurate structure prediction of biomolecular interactions with AlphaFold 3. Nature 630, 493–500.

Bick, R.J., Buja, L.M., Van Winkle, W.B., Taffet, G.E., 1998. Membrane asymmetry in isolated canine cardiac sarcoplasmic reticulum: comparison with skeletal muscle sarcoplasmic reticulum. J. Membr. Biol. 164, 169–175.

Gaburjakova, J., Gaburjakova, M., 2023. Molecular aspects implicated in dantrolene selectivity with respect to ryanodine receptor isoforms. Int. J. Mol. Sci. 24.

Gurrola, G.B., Capes, E.M., Zamudio, F.Z., Possani, L.D., Valdivia, H.H., 2010. Imperatoxin A, a cell-penetrating peptide from scorpion venom, as a probe of Ca-Release channels/ryanodine receptors. Pharmaceuticals 3, 1093–1107.

Gutierrez, J.M., Calvete, J.J., Habib, A.G., Harrison, R.A., Williams, D.J., Warrell, D.A., 2017. Snakebite envenoming. Nat. Rev. Dis. Primers 3, 17063.

Gutierrez, J.M., Ownby, C.L., 2003. Skeletal muscle degeneration induced by venom phospholipases A2: insights into the mechanisms of local and systemic myotoxicity. Toxicon 42, 915–931.

Lai, F.A., Erickson, H.P., Rousseau, E., Liu, Q.Y., Meissner, G., 1988. Purification and reconstitution of the calcium release channel from skeletal muscle. Nature 331, 315–319.

Li, Y., Wei, J., Guo, W., Sun, B., Estillore, J.P., Wang, R., Yoruk, A., Roston, T.M., Sanatani, S., Wilde, A.A.M., Gollob, M.H., Roberts, J.D., Tseng, Z.H., Jensen, H.K., Chen, S.R.W., 2021. Human RyR2 (Ryanodine receptor 2) Loss-of-Function mutations: clinical phenotypes and in vitro characterization. Circ Arrhythm Electrophysiol 14, e010013.

Liang, C., Malik, S., He, M., Groom, L., Ture, S.K., O'Connor, T.N., Morrell, C.N., Dirksen, R.T., 2024. Compound heterozygous RYR1-RM mouse model reveals disease pathomechanisms and muscle adaptations to promote postnatal survival. FASEB J. 38, e70120.

Lomonte, B., 2023. Lys49 myotoxins, secreted phospholipase A(2)-like proteins of viperid venoms: a comprehensive review. Toxicon 224, 107024.

Lomonte, B., Angulo, Y., Rufini, S., Cho, W., Giglio, J.R., Ohno, M., Daniele, J.J., Geoghegan, P., Gutierrez, J.M., 1999. Comparative study of the cytolytic activity of

myotoxic phospholipases A2 on mouse endothelial (tEnd) and skeletal muscle (C2C12) cells in vitro. Toxicon 37, 145–158.
Lomonte, B., Fernandez, J., 2022. Solving the microheterogeneity of Bothrops asper myotoxin-II by high-resolution mass spectrometry: insights into C-terminal region variability in Lys49-phospholipase A(2) homologs. Toxicon 210, 123–131.
Lomonte, B., Gutierrez, J.M., 1989. A new muscle damaging toxin, myotoxin II, from the venom of the snake Bothrops asper (terciopelo). Toxicon 27, 725–733.
Marks, A.R., 2023. Targeting ryanodine receptors to treat human diseases. J. Clin. Investig. 133.
Massimino, M.L., Simonato, M., Spolaore, B., Franchin, C., Arrigoni, G., Marin, O., Monturiol-Gross, L., Fernandez, J., Lomonte, B., Tonello, F., 2018. Cell surface nucleolin interacts with and internalizes Bothrops asper Lys49 phospholipase A(2) and mediates its toxic activity. Sci. Rep. 8, 10619.
Meissner, G., Rios, E., Tripathy, A., Pasek, D.A., 1997. Regulation of skeletal muscle Ca2 + release channel (ryanodine receptor) by Ca2+ and monovalent cations and anions. J. Biol. Chem. 272, 1628–1638.
Montecucco, C., Gutierrez, J.M., Lomonte, B., 2008. Cellular pathology induced by snake venom phospholipase A2 myotoxins and neurotoxins: common aspects of their mechanisms of action. Cell. Mol. Life Sci. 65, 2897–2912.
Mora-Obando, D., Fernandez, J., Montecucco, C., Gutierrez, J.M., Lomonte, B., 2014. Synergism between basic Asp49 and Lys49 phospholipase A2 myotoxins of viperid snake venom in vitro and in vivo. PLoS One 9, e109846.
Ohkura, M., Furukawa, K., Oikawa, K., Ohizumi, Y., 1995. The properties of specific binding site of 125I-radioiodinated myotoxin a, a novel Ca++ releasing agent, in skeletal muscle sarcoplasmic reticulum. J. Pharmacol. Exp. Therapeut. 273, 934–939.
Rodrigues-Simioni, L., Prado-Franceschi, J., Cintra, A.C., Giglio, J.R., Jiang, M.S., Fletcher, J.E., 1995. No role for enzymatic activity or dantrolene-sensitive Ca2+ stores in the muscular effects of bothropstoxin, a Lys49 phospholipase A2 myotoxin. Toxicon 33, 1479–1489.
Sribar, J., Oberckal, J., Krizaj, I., 2014. Understanding the molecular mechanism underlying the presynaptic toxicity of secreted phospholipases A(2): an update. Toxicon 89, 9–16.
Tunwell, R.E., Wickenden, C., Bertrand, B.M., Shevchenko, V.I., Walsh, M.B., Allen, P.D., Lai, F.A., 1996. The human cardiac muscle ryanodine receptor-calcium release channel: identification, primary structure and topological analysis. Biochem. J. 318, 477–487. Pt 2.
Vargas-Valerio, S., Robleto, J., Chaves-Araya, S., Monturiol-Gross, L., Lomonte, B., Tonello, F., Fernandez, J., 2021. Localization of Myotoxin I and Myotoxin II from the venom of Bothrops asper in a murine model. Toxicon 197, 48–54.
Yan, Z., Bai, X., Yan, C., Wu, J., Li, Z., Xie, T., Peng, W., Yin, C., Li, X., Scheres, S.H.W., Shi, Y., Yan, N., 2015. Structure of the rabbit ryanodine receptor RyR1 at near-atomic resolution. Nature 517, 50–55.
Zeng, F., Shen, B., Zhu, Z., Zhang, P., Ji, Y., Niu, L., Li, X., Teng, M., 2013. Crystal structure and activating effect on RyRs of AhV_TL-I, a glycosylated thrombin-like enzyme from Agkistrodon halys snake venom. Arch. Toxicol. 87, 535–545.
Zhou, Q., Wang, Q.L., Meng, X., Shu, Y., Jiang, T., Wagenknecht, T., Yin, C.C., Sui, S.F., Liu, Z., 2008. Structural and functional characterization of ryanodine receptor-natrin toxin interaction. Biophys. J. 95, 4289–4299.